Design and Characterization of a Scalable ion Electrospray Propulsion System

IEPC-2015-149／ISTS-2015-b-149

Presented at Joint Conference of 30th International Symposium on Space Technology and Science, 34th International Electric Propulsion Conference and 6th Nano-satellite Symposium
Hyogo-Kobe, Japan
July 4–10, 2015

David Krejci* and Fernando Mier-Hicks† and Corey Fucetola‡ and Paulo Lozano§
Massachusetts Institute of Technology, Cambridge, MA, 02139, USA

Andrea Hsu Schouten¶
The Aerospace Corporation, El Segundo, CA, 90245, USA

and

Francois Martel‖
Espace Inc, Hull, MA, 02045, USA

Within recent years, the number of Nanosatellites launched has risen rapidly, with increasing use of these platforms in constellation missions. However, a lack of efficient propulsion options with significant Δv capabilities persists, inhibiting the full capabilities of such miniaturized space platforms. At MIT, a MEMS based electrospray thruster has been developed using ionic liquids as propellant. This thruster concept is based on electrostatic extraction and acceleration of charged particles from room temperature molten salts, using porous emitter arrays with emitter densities of 480 emitters per square centimeter. The propellant is passively fed to the emitter by capillary forces only, therefore simplifying the propellant management system and increasing reliability. The implementation of a distal electrode mitigates previously occurring propellant degradation due to electrochemistry, leading to extended lifetime and obviating the need for fast polarity alternation. A single thruster module weights $3.5g$, including acceleration chamber and $1.2cc$ fully-loaded propellant tank, and comes with a footprint of $14.4x14.4mm$ and $14.1mm$ height. These modules present themselves as building blocks for scalable propulsion systems, leading to easy integration and high redundancy. This work presents an integrated propulsion system featuring 8 thrusters firing along a single axis, capable of delivering a thrust of $74\mu N$ at a specific impulse of $> 1150s$ and a total power consumption of less than $1.5W$. This Scalable ion Electrospray Propulsion System (S-iEPS) fits in a 0.2U ($< 200cc$) envelope and weighs less than $100g$ including PPU, and is therefore well adjusted to the stringent requirements imposed by most small satellites, including standardized Cubesats. Since the propulsion system is capable of directly extracting both positively and negatively charged ions, no additional neutralization devices are required. A comprehensive characterization of single thrusters as well as the propulsion unit is presented, allowing determination of vital thruster parameters such as specific impulse, total impulse generated by the propulsion module and the Δv capability enabled by this propulsion unit for selected mission configurations.

*Postdoctoral Scholar, Department of Aeronautics and Astronautics, krejci@mit.edu.
†PhD candidate, Department of Aeronautics and Astronautics
‡Postdoctoral Scholar, Department of Aeronautics and Astronautics
§Professor, Department of Aeronautics and Astronautics, plozano@mit.edu
¶Research Scientist, Propulsion Science Department, andrea.g.hsu@aero.org
‖President, fm@space.mit.edu.

I. Introduction

In recent years, Cubesats have transformed from purely educational and technology demonstration tools into platforms for demanding scientific and commercial missions. The combination of relatively low launch costs, rapid development cycles and the possibility for constellations at low cost, featuring redundancy, high temporal resolution and flexibility, have resulted in a fast growing number of Nanosatellite missions.[1] However, to fully exploit these future capabilities, like advanced constellation missions, Nanosatellites are in dire need of autonomous propulsion systems, complying with the stringent power, mass and volume requirements imposed. The propulsion system presented in this work is a highly efficient electrostatic propulsion system with fully passive propellant management, complying with mass, volume and power requirements of even single Cubesats, with a minimum specific impulse of 1200s. In addition, the thrusters are designed to be highly modular, and can be easily adapted to specific mission requirements, by changing the number of thrusters, thruster location or orientation.

II. Ionic liquid electrospray propulsion

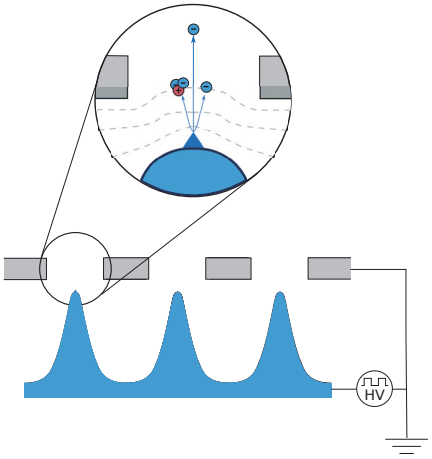

Figure 1. Electrospray principle with charged particle extraction from Taylor cone on top of porous emitter structures

Ionic liquids are room temperature molten salts, composed of positive and negative charges and feature negligible vapor pressure,[2,3] two properties that make them highly suitable for space propulsion applications. In the thruster presented, the propellant is fed passively, by capillary forces, to an array of sharp emitter structures. When applying a potential difference between the liquid and a counter-electrode, electrostatic pull is counteracted by surface tension, forming a so-called "Taylor cone",[4] as indicated in Fig. 1. When surpassing a certain potential threshold, ions are extracted from the cone's apex.[5,6] These ions are then accelerated by the applied potential to high exhaust velocities, producing thrust at highly efficient propellant utilization. Due to the unique nature of the propellant, both positive and negative ions can be extracted, allowing for polarity alternation and neutralization by firing pairs of thrusters at opposite polarity.
The ability of ion emission for ionic liquid electrospray thrusters has been experimentally shown.[7–11] However, instead of extracting ions exclusively, experimental investigations have also shown the existence of larger clusters and droplets in the beam,[7,12] resulting in a higher mean particle mass of the expelled exhaust, therefore lowering the specific impulse. The impact of solvated ions and droplets in the exhaust beam is thoroughly discussed in Ref.[13]
This kind of electrostatic propulsion principle is generally featuring high specific impulse, but produces thrust levels that are below typical mission requirements. Researchers have therefore attempted to operate multiple emitters in parallel to increase thrust without performance penalty.[14–20]

III. S-iEPS thruster

At the Space Propulsion Laboratory at the Massachusetts Institute of Technology, a highly miniaturized thruster has been developed.[18,21] This thruster features a porous glass emitter with 480 emitter tips arranged in a square pattern.[22] This emitter chip is housed in a silicon DRIE manufactured package, guaranteeing exact alignment of the emitter tips with the corresponding extractor holes, while providing electrical insulation between the emitter and the extractor layer. An exploded view of the thruster package is shown in Fig. 2 on the left hand side.

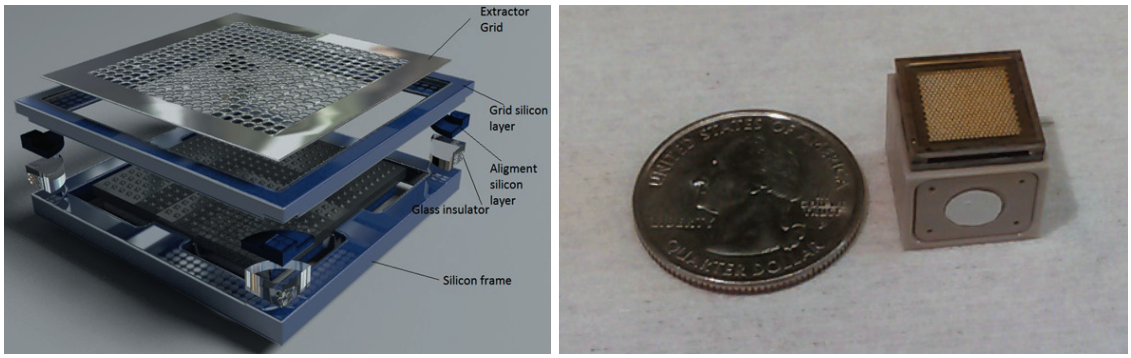

Figure 2. Left: Exploded view of the emitter to extractor packaging for the porous glass emitter chip featuring 480 individual emitter tips. Right: Fully packaged thruster including 480 emitter array, acceleration chamber and passive propellant management system featuring 1.2cc tank volume

The thruster head is then assembled on top of the propellant tank, with propellant being passively fed from the liquid reservoir, through porous medium, to the backside of the emitter chip via a propellant port in the silicon packaging. High voltage is contacted to the propellant using a distal electrode with high internal surface area[23] inside the propellant tank. The concept of contacting the high voltage at a remote distance from the emission site was motivated by increasing the contact surface area to avoid local potential differences from exceeding the electrochemical window of the ionic liquid propellant.[23] By doing so, previously encountered electrochemical decomposition effects leading to limited emitter lifetime, could be avoided. The fully packaged thruster, including tank volume for up to $1ml$ of propellant features a footprint of $14.4x14.4mm^2$ and $14.1mm$ height, with $< 3.5g$ wet weight. Fig. 2 right hand side shows a fully packaged S-iEPS thruster. The quasi cubic form factor of the thruster allows for easy scalability and easy adaption to mission requirements concerning thruster location, thrust orientation and number of thrusters.

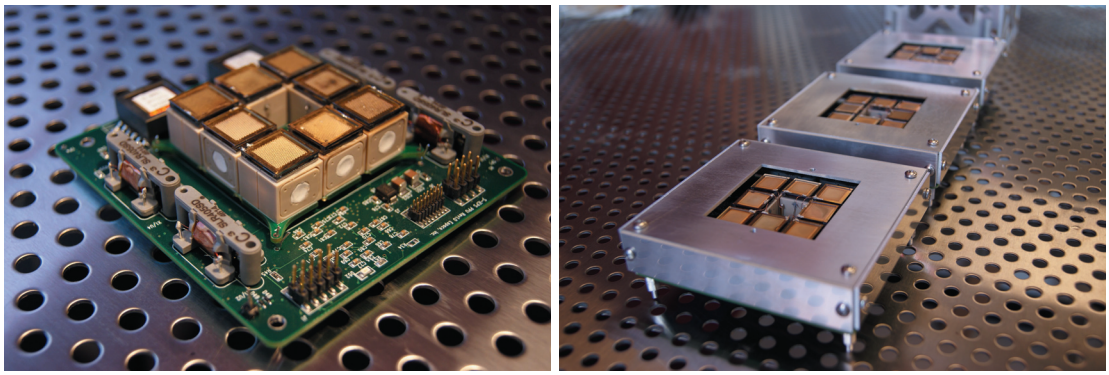

Figure 3. NASA MEP S-iEPS propulsion module featuring 8 thrusters and PPU, without (left) and with (right) protective enclosure for testing.

The propulsion module features 8 centrally located thrusters arranged in a square pattern mounted to a dedicated PCB, including a resistive heater for active temperature control. This thruster module is attached to the power processing unit (PPU) PCB in a planar way, with main electrical components, such as high voltage transformers and polarity switching components, allocated around the thrusters, guaranteeing minimal packaging volume. Fig. 3 shows the S-iEPS module including PPU and 8 thrusters. Key physical

Metric	Measured value
Dry mass	$\sim 95g$
Dimensions	$96x96x21mm$
Average power consumption	$\leq 1.5W$
PPU peak efficiency	$\sim 88.5\%$

Table 1. S-iEPS module physical and PPU characteristics

parameters of the propulsion module are summarized in Table 1. Note that propulsion module characteristics related to thruster performance are listed in section VI, Table 2.

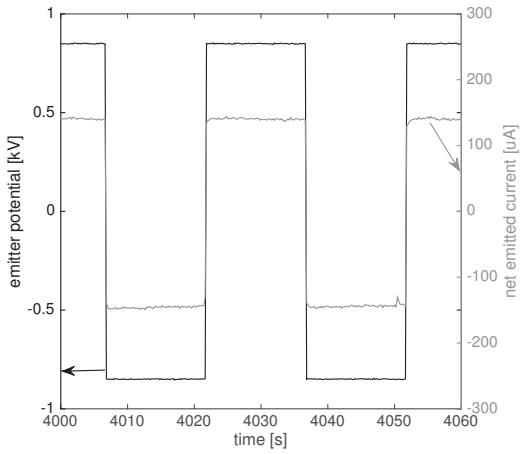

Figure 4. Detail of applied emitter potential and emitted current for 30s polarity alternation period

IV. Thruster operation

To guarantee electrochemical stability of the propellant, it has been suggested to operate ionic liquid electrospray emitters at alternating polarities.[21] Whereas alternation frequencies of approximately $1Hz$ were proposed for conductive emitters, contacting the high voltage potential to the liquid in the vicinity of the emission site, the incorporation of the distal electrode allows for significantly decreased polarity alternation periods. In this work, polarity alternation periods of $10 - 30s$ were used to avoid asymmetric depletion of charge within the propellant reservoir. However, successful thruster operation in single polarity for over $40h$ has been shown previously for similar thruster configurations. Fig. 4 shows typical applied potential and emitted current test details for a $30s$ polarity alternation period.
Before reaching stable emission, the emitters typically require a conditioning phase at initial startup. During this phase, emitted currents are low, necessitating high emitter potentials to achieve emission, when compared to the operational conditions found after startup. It is anticipated that during this conditioning time, electrostatic pull of the liquid enhances final distribution of the propellant within the porous emitter array and increased potentials are required to overcome repelling surface forces. After this initial conditioning phase, emission current is generally stable and can be easily controlled over a wide range of emission currents by varying the applied potential.

V. Thruster testing

A. Single thruster test results

Fig. 5 left hand side shows a typical emission characteristic profile for a single S-iEPS thruster. The data shown is an average from three successive recordings, applying emitter voltage in a triangular profile in time

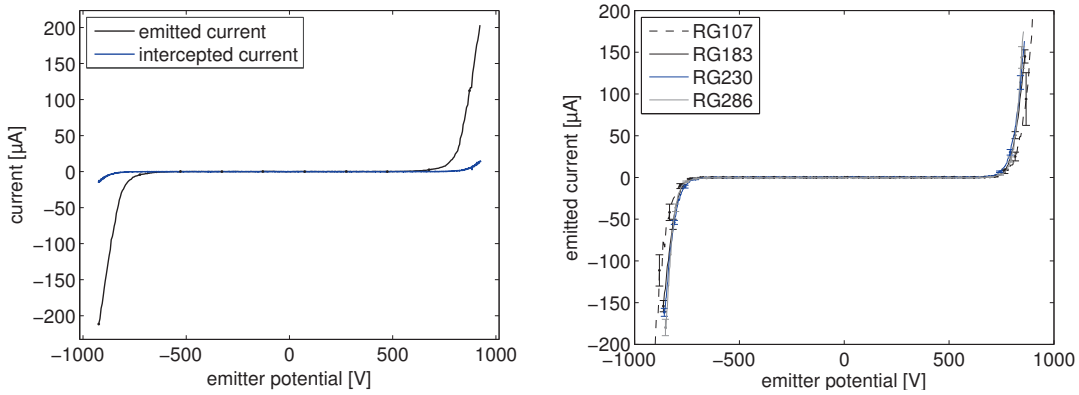

Figure 5. Emitted and intercepted current as a function of applied emitter potential (left) and emitter-to-emitter variability of emitted current (right)

from negative to positive values and vice-verse. Shown are the emitted current, that is the measured supply current drawn by the emitter, and the intercepted current, that is the current measured from the extractor electrode to ground. Relative interception is defined as the ratio of intercepted to emitted current. Relative interception at nominal emission current of $150\mu A$ is $\sim 5\%$ in both polarities for the emitter shown. The emission data in Fig. 5 shows the very good symmetry of emission regarding polarity.

Fig. 5 right hand side compares the emission behavior of multiple thrusters, recorded after the conditioning phase to study emitter to emitter variability. Small variability is important to avoid unequal emission currents drawn by different emitters when operating multiple emitters in parallel as proposed in the S-iEPS design. The data in Fig. 5 however indicates emitter to emitter variance to be small, and is generally anticipated to be smaller than tip to tip variance within individual emitter arrays.

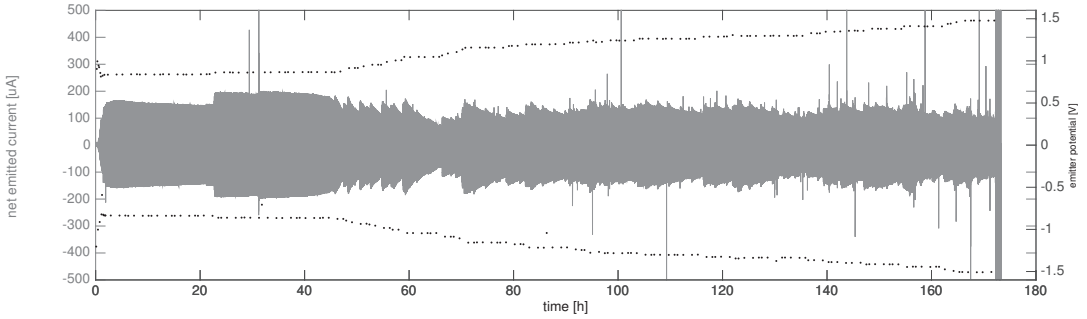

Figure 6. Net emitted current and applied emitter potential for a $172h$ duration test

Lifetime tests have been performed on single S-iEPS thrusters using lab power supplies (Matsusada AP-3B1-L2) at a base pressure of $< 5 * 10^{-6} Torr$. These tests typically exhibit three different operational stages: The warm up phase described in section IV which is typically completed at $< 2h$, followed by a period of constant emission behavior. After approximately $40 - 70h$, a decay in emission current is noticed, necessitating periodic increases of the applied emitter potential to maintain a constant emission current level of $\pm 150\mu A$. Throughout these tests, applied potential as well as emitted and intercepted currents were measured to monitor the emitter status. Fig. 6 shows a comparison of the net emission current, that is the intercepted current subtracted from the emitted current, and the corresponding applied emitter potential. The first thing to notice are the isolated features of high current, which are attributed to discharges between emitter tips and the extractor. These discharges leave residue of decomposed ionic liquids, and in some instances were found strong enough to fully destroy individual emitters, leading to a recovery of the emission properties in case of failed emitters.

As mentioned earlier, current decay observed after approximately $50h$ of operation necessitated adjustments in the applied emitter potential.

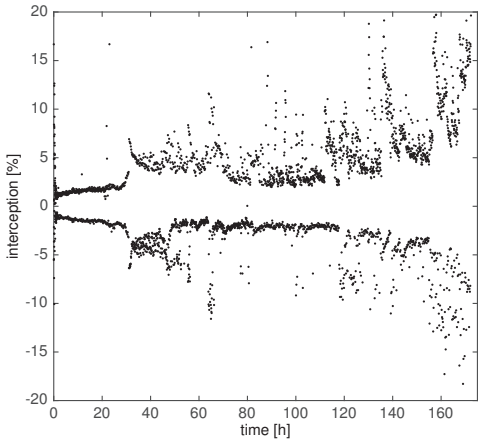

Figure 7. Relative interception during $172h$ test

Fig. 7 shows the timely evolution of the relative interception. Note that due to the polarity alternation operation, single data points show diverging behavior caused by division by small values during switching. Nevertheless, this data shows a steadily increasing interception on a long duration scale, indicating an increasing number of emitters that formed conducting "bridges" to the extractor, most likely a result of propellant decomposition during discharges. In addition, steadily increasing the emitter potential after $50h$ into the test led to increased stressing of the emission site, increasing the possibility for off-axis emission and could thus have contributed to the increase in interception. The significant increase in relative interception shown after $160h$ ultimately led to thruster failure due to electrical shortening between emitter and extractor, as indicated by the sudden increase in current shown in Fig. 6, limited only by the set limit of the power supply.

Integrating the net emitted current for the test shown in Fig. 6 allows us to determine an average charge to mass ratio of the exhaust plume, in conjunction with the known total propellant consumption, from gravimetric measurement of the thruster weight before and after the test, with carefully avoiding humidity intake by the propellant before weighting. For a total consumed propellant mass of $0.6306g$, the average charge to mass ratio is calculated as $q/m = 125C/g$. Given the significant changes in emitter potential, it is obvious that the approximation of constant charge to mass ratio introduces an overestimation of q/m in the beginning of the test, and according underestimation during the final stages of the test. However, it allows to derive an average value for the specific impulse of $I_{sp} = 1717s$. As the specific impulse scales with $I_{sp} \sim \sqrt{V_e}$, the assumption of constant charge to mass ratio throughout the test leads to specific impulse smaller than the average value in the early stages of the test, whereas specific impulse increased and surpasses the average value with increasing test duration.
Tests terminated before current decay was observed allowed to determine the specific impulse achieved at nominal operation voltages of $< 900V$. The specific impulse of the S-iEPS at nominal operation conditions for the first $60h$ after startup conditioning, without increased emission potential, was found to be $I_{sp} = 1167.5 \pm 60.7s$.

B. S-iEPS propulsion module test results

Tests have been performed using a pair of thrusters operated by the highly efficient S-iEPS power processing unit. Fig. 8 shows the current traces of two S-iEPS thrusters fired by the S-iEPS PPU in opposite polarities at a polarity alternation period of $20s$, excluding idle times due to voltage decay necessary before switching. As the S-iEPS does not allow for direct current measurements of the high voltage side, currents have been measured with external, galvanically isolated, laboratory current monitors. This test shows that the PPU is able to operate two thrusters firing at opposite polarity with slightly different emission characteristics.

The unique feature of ionic liquid electrospray thrusters to emit charged particles of both polarities allows for direct neutralization of the beam and the satellite potential by parallel firing thrusters in opposite polarity. In the S-iEPS design, extractors of both polarities are interconnected and floating with respect to

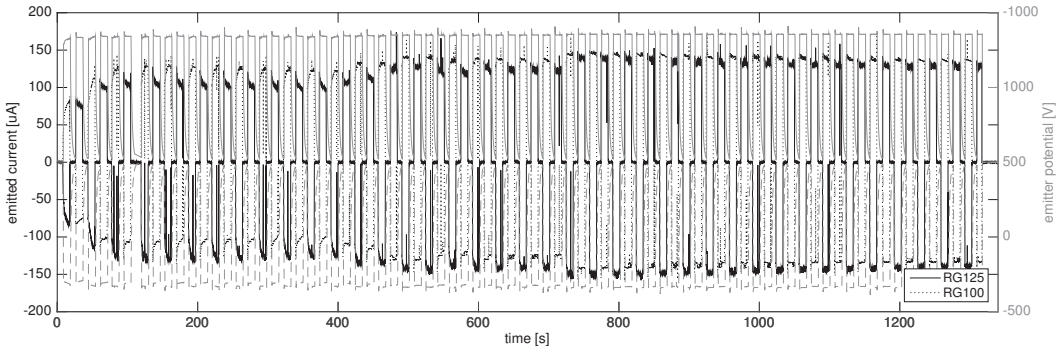

Figure 8. Potential and current traces for a pair of S-iEPS thrusters operated by the S-iEPS PPU

the PPU ground. Applying positive and negative potentials to the two groups of emitters allows extraction of charges with respect to this floating extractor potential. In case of potential drift of the PPU ground, this would lead to an increased potential drop experienced by the emitters of opposite polarity, increasing the emitted current in this polarity and therefore counteracting any potential drift.

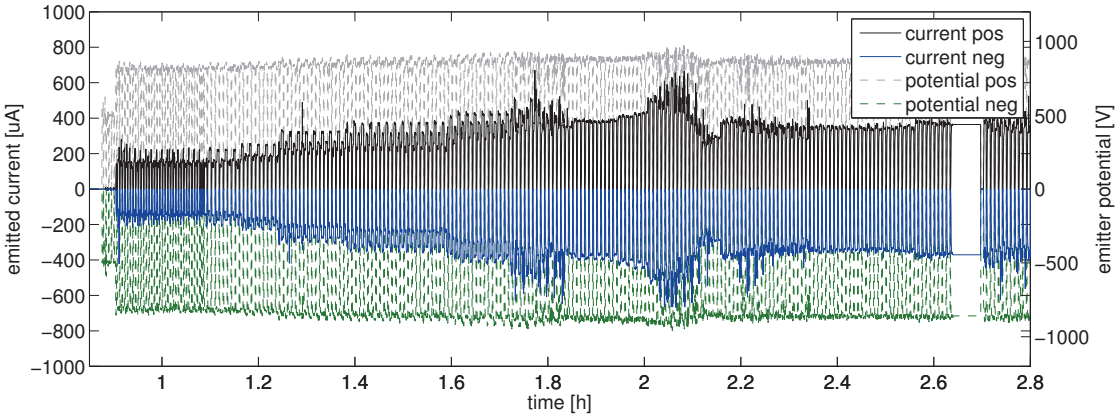

Figure 9. Potential and current traces for a battery powered, floating prototype PPU during startup

To validate this inherent neutralization design, an S-iEPS unit was tested using a battery powered, floating PPU. The recorded thruster potentials and emitted currents of this test are plotted in Figure 9. It should be noted that this test was conducted using pristine, unfired thrusters, with emitters typically experiencing the largest emitter-to-emitter variance during this conditioning phase. This test can therefore be regarded as a worst case scenario in terms of potential mismatch of emitted currents. However, the data shown in Fig. 9 clearly validates the neutralization approach, with stable, symmetric emission currents observed in both polarities. To avoid depletion of the batteries, the PPU was switched to a laboratory power supply at approximately $2.65h$ after test start. This test shows that the PPU is able to operate groups of thrusters firing at opposite polarity even during startup of the thrusters, where emitters are prone to exhibit unstable emission behavior with increased emitter-to-emitter variance. Potential drift caused by this asymmetry is equilibrated by a shift in emission potential in favor of the opposite emission polarity. In this test, special care was taken to minimize any potential leakage currents at mounting contacts of the PPU. In addition, the principle of operating a pair of fully floating thrusters has been verified using a magnetically levitated, hence leakage current free, setup as described in Ref.[24]

Fig. 10 shows the time traces of applied potentials and emitted currents in positive and negative polarities during a $52h$ test for a full S-iEPS module. Note that a prototype PPU was again used for this test. This PPU features less efficiency in the high voltage conversion, but allowed for advanced thruster monitoring, such as direct current measurements on the high voltage side.

In this test, emitters were started up individually. However, it was found that one of the emitters ceased to emit even at increased voltages, so it was decided to disconnect another thruster in the opposite polarity, and conduct the test with three emitters per polarity. The plot shows the conditioning phase, much like the conditioning of single thrusters discussed in previous chapters, followed by stepwise increase of the emitted currents up to the nominal $150\mu A$ per thruster. In this configuration, 3 thrusters were operated in parallel in each polarity, so the nominal current accumulates to $450\mu A$ per polarity, or $0.9mA$ total. During this test, the propulsion module was fired for approximately $51h$ at nominal emission current of $450 \pm 25\mu A$. During this time, the propulsion module exhibited no signs of current decay, coinciding with data on single thrusters presented in section A. In addition, symmetry of emission of succeeding emission periods show the uniformity of emission of the two thruster groups with respect to each other.
After approximately $14h$ of firing, emission was halted for an hour to investigate restart capability. No impact of the idle time on thruster behavior was noticed upon restart.
After approximately $52h$, the test was terminated due to an electrical short in one of the emitters.

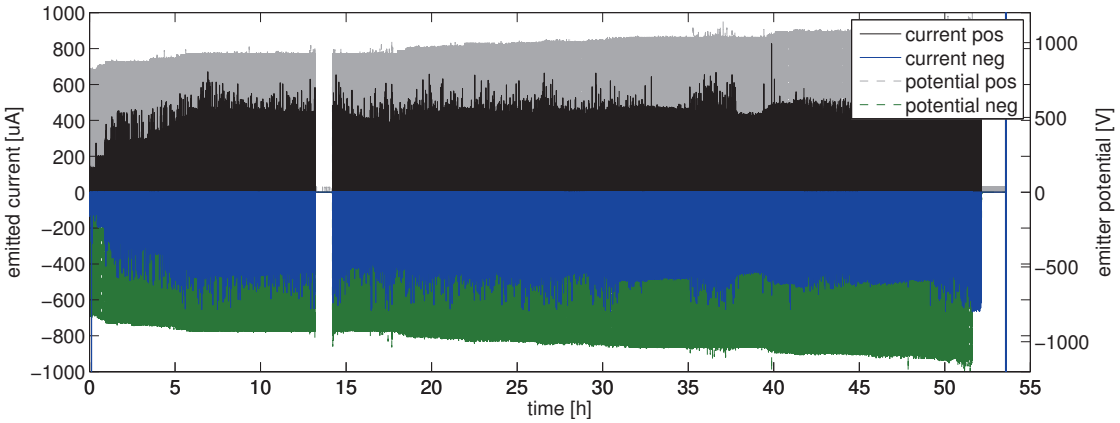

Figure 10. Full module test with 8 S-iEPS thrusters: potentials and currents with prototype PPU

C. S-iEPS thruster module thrust test

Thrust tests have been conducted at Propulsion Science Department at The Aerospace Corporation. The thrust stand consisted a torsional balance with 1 μN sensitivity. In this configuration, the displacement of the suspended arm is directly correlated to the thrust using a spring constant that was determined for the exact measurement setup including wiring. A detailed description of the experimental setup, calibration and sensitivity characterization can be found in Ref.[25] Figure 11 left hand side shows the S-iEPS propulsion unit mounted to the thrust stand before firing. Due to a PPU malfunction during startup, the two polarities of the thruster were powered directly by two lab power supplies, with incorporated polarity alternation.
After successful startup of the propulsion unit, thrust measurements were taken while the emitter potentials were increased in steps of $25V$ over the duration of approximately two hours to ramp up the emission current to the nominal level of $600\mu A$ per polarity, or $1.2mA$ total. The measured thrust as a function of emitted current is shown in Fig. 11 on the right hand side. It should be noted that intercepted current was not measured during this test, and net emitted current was therefore smaller than current displayed.
During the test a current asymmetry between polarities was noticed of approximately $150\mu A$, potentially indicating an inactive thruster throughout the test.
The thrust data plotted comprises of three measurements taken at $1.5h$, $5h$ and $7h$ after startup. Not change in measured thrust during this time period was noticed. The measured thrust scales linear with current, as anticipated, with maximum thrust of $74 \pm 3.7\mu N$ measured at an emission current of $1.175mA$. The plot in Fig. 11 shows linear interpolation to $1.2mA$, yielding a thrust of $81.5 \pm 4.1\mu N$ at a total current of $1.2mA$. The net emitted current was however smaller than the current stated in this discussion due to the intercepted current, unknown in this test.
The thruster was operated for a total of approximately $39.5h$, including the two hour startup phase at the maximum emission current of $1175\mu A$ total.

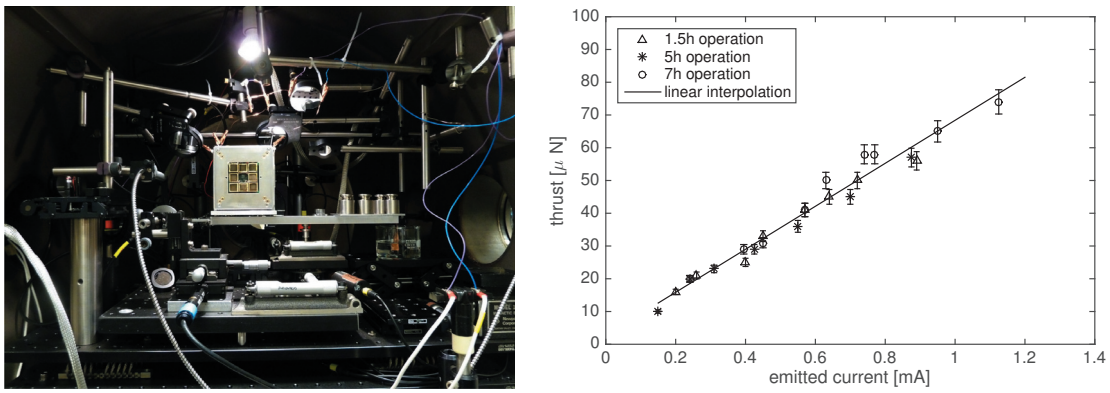

Figure 11. S-iEPS propulsion unit mounted to thrust balance (left), and measured thrust as a function of current (right)

VI. Discussion and Conclusion

This paper presents the design and test results of the Scalable-ion Electrospray Propulsion system, an ionic liquid MEMS based electric propulsion system for Nanosatellites. The highly miniaturized propulsion system consists of eight individual thrusters that can be easily reconfigured or scaled to mission requirements. Each of the thruster consists of an emitter array featuring 480 emitter tips, packaged within a $1cm^2$ surface area, manufactured with MEMS processes. Ionic liquid propellant is passively supplied to each of these emitters from individual tanks. Due to the unique features of the propellant, the thrusters can emit charged particles in both polarities, and are typically operated in a low frequency polarity alternation scheme, to avoid asymmetric depletion of charge within the propellant reservoir.

Section A presents experimental data showing symmetrical emission characteristics at small relative interception, and current stability of single S-iEPS thrusters once fully conditioned. Test data collected during a long duration test is presented, allowing determination of an average charge to mass ratio and therefore an average specific impulse of $I_{sp} = 1717s$. Initial specific impulse at nominal operation is found as $I_{sp} = 1167.5 \pm 60.7s$.

Section B shows initial tests of S-iEPS thrusters operated by the highly efficient S-iEPS PPU. This PPU features a peak efficiency of $\sim 88.5\%$. Experimental data recorded for a startup of a S-iEPS propulsion unit using a floating, battery PPU validated the ability to counteract asymmetries in emission current without PPU charging to potentials influencing emission.

These initial test results are succeeded by presentation of a firing test of a full S-iEPS propulsion unit, operated by a prototype PPU allowing for direct high voltage side current measurements. The test presented shows that the full thruster array experiences similar conditioning behavior as found for single emitters, and that multiple S-iEPS thrusters can be stably fired in parallel. The S-iEPS propulsion unit was fired for $52h$ at nominal emission current of $150\mu A$ per emitter. The module was operated in groups of three thrusters firing in parallel per polarity and showed stable emission, good emission symmetry and no signs of potential drift. As with single thrusters, the propulsion module showed stable emission currents for constant potential after warmup.

Thrust measurements conducted at The Aerospace Corporation verified thrust to scale linear with current in a first approximation. Maximum thrust measured was $74 \pm 3.7\mu N$ at a total emission current of $1.175mA$, despite current asymmetry encountered during this test at high emission currents. This asymmetry potentially indicates an inactivity of one emitter throughout the test. Intercepted current was not measured during this test, leading to a slight overestimation of the emitted current during the thrust measurements. Extrapolation of thrust data to nominal emission current of $1.2mA$ yields a thrust of $81.5 \pm 4.1\mu N$, not considering interception.

The full S-iEPS unit was fired at The Aerospace Corporation at nominal current for $39.5h$.

Metric	Measured
Measured thrust at $1.125mA$	$74 \pm 3.7\mu N$
Interpolated thrust at $1.2mA$	$81.5 \pm 4.1\mu N$
Specific impulse at initial nominal operation voltage	$1167.5s \pm 60.7s$
Average specific impulse (172h average)	$1717s$
Experimental lifetime (single emitter)	$172h$

Table 2. S-iEPS module performance characteristics

Acknowledgments

This work was supported by NASA through contract No. NNL13AA12C under NASA's Game Changing Development program of the Space Technology Mission Directorate (STMD).

References

[1]D. Selva and D. Krejci, "A survey and assessment of the capabilities of cubesats for earth observation," *Acta Astronautica*, vol. 74, no. 0, pp. 50 – 68, 2012.

[2]D. H. Zaitsau, G. J. Kabo, A. A. Strechan, Y. U. Paulechka, A. Tschersich, S. P. Verevkin, and A. Heintz, "Experimental vapor pressures of 1-alkyl-3-methylimidazolium bis(trifluoromethylsulfonyl)imides and a correlation scheme for estimation of vaporization enthalpies of ionic liquids," *The Journal of Physical Chemistry A*, vol. 110, no. 22, pp. 7303–7306, 2006. PMID: 16737284.

[3]E. F. Smith, F. J. M. Rutten, I. J. Villar-Garcia, D. Briggs, and P. Licence, "Ionic liquids in vacuo: analysis of liquid surfaces using ultra-high-vacuum techniques," *Langmuir*, vol. 22, no. 22, pp. 9386–9392, 2006. PMID: 17042558.

[4]G. Taylor, "Disintegration of water drops in an electric field," *Royal Society of London Proceedings Series A*, vol. 280, pp. 383–397, 1964.

[5]M. Gamero-Castaño and J. Fernández de la Mora, "Direct measurement of ion evaporation kinetics from electrified liquid surfaces," *The Journal of Chemical Physics*, vol. 113, pp. 815–832, 2000.

[6]I. Romero-Sanz, R. Bocanegra, J. Fernandez de la Mora, and M. Gamero-Castaño, "Source of heavy molecular ions based on taylor cones of ionic liquids operating in the pure ion evaporation regime," *Journal of Applied Physics*, vol. 94, pp. 3599–3605, 2003.

[7]P. Lozano and M. Martinez-Sanchez, "Experimental measurements of colloid thruster plumes in the ion-droplet mixed regime," in *38th AIAA/ASME/SAE/ASEE Joint Propulsion Conference & Exhibit*, American Institute of Aeronautics and Astronautics, 2015/04/06 2002.

[8]P. Lozano, M. Martnez-Sánchez, and J. M. Lopez-Urdiales, "Electrospray emission from nonwetting flat dielectric surfaces," *Journal of Colloid and Interface Science*, vol. 276, no. 2, pp. 392 – 399, 2004.

[9]P. Lozano and M. Martínez-Sánchez, "Ionic liquid ion sources: characterization of externally wetted emitters," *Journal of Colloid and Interface Science*, vol. 282, no. 2, pp. 415 – 421, 2005.

[10]Y.-H. Chiu, B. L. Austin, R. A. Dressler, D. Levandier, P. T. Murray, P. Lozano, and M. M. Sanchez, "Mass spectrometric analysis of colloid thruster ion emission from selected propellants," *Journal of Propulsion and Power*, vol. 21, pp. 416–423, 2015/05/05 2005.

[11]P. C. Lozano, "Energy properties of an emi-im ionic liquid ion source," *Journal of Physics D: Applied Physics*, vol. 39, no. 1, p. 126, 2006.

[12]C. Ryan, A. Daykin-Iliopoulos, J. Stark, A. Salaverri, E. Vargas, P. Rangsten, S. Dandavina, C. Ataman, S. Chakraborty, D. Courtney, and H. Shea, "Experimental progress towards the microthrust mems electrospray electric propulsion system," in *33rd Joint Propulsion Conference and Exhibit*, 2013.

[13]P. C. Lozano, *Studies on the Ion-Droplet Mixed Regime in Colloid Thrusters*. PhD thesis, Department of Aeronautics Ans Astronautics, Massachusetts Institute of Technology, 2003.

[14]C. Spindt, "Microfabricated field-emission and field-ionization sources," *Surface Science*, vol. 266, no. 1–3, pp. 145 – 154, 1992.

[15]F. Pranajaya and M. Cappelli, "Development of a colloid micro-thruster for flight demonstration on the emerald nanosatellite," in *37th Joint Propulsion Conference and Exhibit*, American Institute of Aeronautics and Astronautics, 2015/04/06 2001.

[16]R. Krpoun and H. R. Shea, "Integrated out-of-plane nanoelectrospray thruster arrays for spacecraft propulsion," *Journal of Micromechanics and Microengineering*, vol. 19, no. 4, p. 045019, 2009.

[17]G. B.L.P., *A Fully Microfabricated Two-Dimensional Electrospray Array with Applications to Space Propulsion*. PhD thesis, Massachusetts Institute of Technology, 2007.

[18]D. G. Courtney, H. Q. Li, and P. Lozano, "Emission measurements from planar arrays of porous ionic liquid ion sources," *Journal of Physics D: Applied Physics*, vol. 45, no. 48, p. 485203, 2012.

[19]K. Tang, Y. Lin, D. W. Matson, T. Kim, and R. D. Smith, "Generation of multiple electrosprays using microfabricated emitter arrays for improved mass spectrometric sensitivity," *Analytical Chemistry*, vol. 73, no. 8, pp. 1658–1663, 2001. PMID: 11338576.

[20]S. Arscott, S. Le Gac, C. Druon, P. Tabourier, and C. Rolando, "Micromachined 2d nanoelectrospray emitter [mass spectrometer applications]," *Electronics Letters*, vol. 39, pp. 1702–1703, Nov 2003.

[21]P. Lozano and M. Martínez-Sánchez, "Ionic liquid ion sources: suppression of electrochemical reactions using voltage alternation," *Journal of Colloid and Interface Science*, vol. 280, no. 1, pp. 149 – 154, 2004.

[22]C. Coffman, L. Perna, H. Li, and P. C. Lozano, "On the manufacturing and emission characteristics f a novel borosilicate electrospray source," in *49th AIAA/ASME/SAE/ASEE Joint Propulsion Conference*, 2013.

[23]N. Brikner and P. C. Lozano, "The role of upstream distal electrodes in mitigating electrochemical degradation of ionic liquid ion sources," *Applied Physics Letters*, vol. 101, no. 19, pp. –, 2012.

[24]F. Mier-Hicks and P. C. Lozano, "Thrust measurements of ion electrospray thrusters using a cubesat compatible magnetically levitated thrust balance," in *34th International Electric Propulsion Conference*, 2015.

[25]A. Hsu Schouten, E. Beiting, and T. Curtiss, "Performance of a torsional thrust stand with 1 μn sensitivity," in *34th International Electric Propulsion Conference*, 2015.